

Article

Uncertainty Assessments of Satellite Derived Rainfall Products

Margaret Kimani *, Joost Hoedjes and Zhongbo Su

Faculty of Geo-Information Science and Earth Observation, University of Twente, P.O Box 217,
7500 AE Enschede, The Netherlands; j.c.b.hoedjes@utwente.nl (J.H.); z.su@utwente.nl (Z.S.)

* Correspondence: m.w.kimani@utwente.nl; Tel.: +31-53-487-4444

Abstract: Accurate and consistent rainfall observations are vital for climatological studies in support of better planning and decision making. However, estimation of accurate spatial rainfall is limited by sparse rain gauge distributions. Satellite rainfall products can thus potentially play a role in spatial rainfall estimation but their skill and uncertainties need to be understood across spatial-time scales. This study aimed at assessing the temporal and spatial performance of seven satellite products (TARCAT (Tropical Applications of Meteorology using SATellite and ground-based observations (TAMSAT) African Rainfall Climatology And Time series), Climate Hazards Group InfraRed Precipitation with Station data (CHIRPS), Tropical Rainfall Measuring Mission (TRMM-3B43), Climate Prediction Center (CPC) Morphing (CMORPH), the Precipitation Estimation from Remotely Sensed Information using Artificial Neural Networks- Climate Data Record (PERSIANN-CDR), CPC Merged Analysis of Precipitation (CMAP) and Global Precipitation Climatology Project (GPCP) using gridded (0.05°) rainfall data over East Africa for 15 years (1998–2012). The products' error distributions were qualitatively compared with large scale horizontal winds (850 mb) and elevation patterns with respect to corresponding rain gauge data for each month during the 'long' (March–May) and 'short' (October–December) rainfall seasons. For validation only rainfall means extracted from 284 rain gauge stations were used, from which qualitative analysis using continuous statistics of Root Mean Squared Difference, Standard deviations, Correlations, coefficient of determinations (from scatter plots) were used to evaluate the products' performance. Results revealed rainfall variability dependence on wind flows and modulated by topographic influences. The products' errors showed seasonality and dependent on rainfall intensity and topography. Single sensor and coarse resolution products showed lowest performance on high ground areas. All the products showed low skills in retrieving rainfall during 'short' rainfall season when orographic processes were dominant. CHIRPS, CMORPH and TRMM performed well, with TRMM showing the best performance in both seasons. There is need to reduce products' errors before applications.

Keywords: satellite; rainfall; estimates; rain gauge; uncertainties; topography; seasonality; East Africa

1. Introduction

Accurate rainfall measurements are very important for many applications, such as hydrological modelling, agricultural practices and climate studies. Rain gauge measurements provide the most direct measurement of rainfall, but rain gauge networks are often spatially and temporally limited [1]. Satellite derived rainfall products may complement sparse rain gauge data, and have the advantage of a wide and consistent coverage [2, 3]. Their estimates are mainly derived from thermal infrared (IR) sensors on board geostationary satellites, and passive and active microwave (MW) sensors on board low earth orbiting satellites. Some products combine the IR and MW based products, thus taking advantage of the high temporal resolution of IR platforms, and the better accuracy in rainfall estimation of MW sensors. However, such indirect rain rate estimation approaches have inherent uncertainties. Most satellite derived rainfall products have been

validated globally and regionally [4, 5]. However, there is still large discrepancies with ground observations at subregional level, where this data is applied [6]. Furthermore, the uncertainties of these products have a seasonal and climatic dependence [7]. It is therefore important to ascertain their uncertainties at a regional scale before choosing the most appropriate product for a particular application. The regional aspects especially over mountainous areas, modulate rainfall occurrence and variability. An example is work done by Diem et al [8] who have assessed three high resolution products over western Uganda. These were the African Rainfall Climatology, version 2 (ARC2); the National Oceanographic and Atmospheric Administration Climate Prediction Center (NOAA-CPC) African Rainfall Estimation Algorithm, version 2 (RFE2); and the Tropical Rainfall Measuring Mission (TRMM 3B42v7)), which were compared at daily, monthly and seasonal time scales for a period of ten years (2001-2010) against ground observations. Their results showed poor performance of all the products over mountainous areas and their errors were attributed to orographic effects. A similar study was carried out by Mashingia et al [9] over Northeast Tanzania. They validated two gauge corrected high resolution satellite rainfall products derived from combined infrared and passive microwave sensors. The validation was done using observations from rain gauge stations network. The products showed underestimations over areas of high elevation, which according to the authors was related to algorithm use of infrared sensor that considers warm clouds to be non-precipitating. However, warm orographic processes do occur. Dinku et al [10] carried a study over Eastern Africa region and explored the effect of mountains and arid climates on four satellite rainfall estimates products performances. The products evaluated include African Rainfall Climatology (ARC), the passive-microwave-only product CMORPH (the the Climate Prediction Center Morphing technique) and two products, the RFE algorithm and TRMM-3B42), which combine data from both infrared and passive-microwave sensors. The result showed an underestimation of the satellite rainfall products, which they associated to warm orographic processes. Results further showed the single infrared sensor ARC algorithm, had the lowest performance over those high ground areas. They attributed this low performance to its infrared assignment of warm cloud as “not precipitating”. Most of the studies, especially those carried out over equatorial Africa (e.g. East Africa), have concentrated on high resolution satellite data for hydrological inputs. Long term assessments, which are very important for e.g. climate studies and water resource management applications, have received little attention. To assess the satellite products performance, one requires good coverage and consistent reference data. Although the GPCC (Global Precipitation Climatology Centre) gauge network is widely used to validate satellite products and shows good performance[11] their coarse resolution (0.5o) requires local corrections before the data can be used in applications [12]. A higher resolution dataset is required to characterize the small distance local effects especially over East Africa. The Intergovernmental Authority on Development (IGAD) Climate Prediction and Applications Center (ICPAC), in collaboration with regional meteorological organizations, have developed a gridded rainfall data (0.05°) <http://www.icpac.net/>. The data covers the greater horn of Africa, and includes all available rain gauge measurements that have been quality controlled over the region from meteorological agencies. Recent comparison of these data with GPCC shows close correspondence [13]. Furthermore, the gridded ICPAC dataset includes data from more rain gauges than what is used in the GPCC data, which fills the gaps and make the dataset more preferable for use for sub regional applications.

East Africa experiences two main rainfall periods. The first occurs during the months of March, April and May, and the second during the months of October, November and December. These two rainy seasons are popularly referred as the long and short rainfall seasons, respectively. The rainy seasons are driven by the seasonal cycle of the Inter-Tropical Convergence Zone (ITCZ). Nicholson [14] studied the Turkana Jet climatology over the region, and its links to regional aridity. He used ERA-Interim wind data at high temporal resolution (6 hours). His results showed that the direction and the strength of tropospheric winds may enhance wetness or dryness over the region. He associated the Turkana jet to aridity over northeast Kenya, Somalia and southern Ethiopia.

Although this study was carried out using high temporal resolution data sets, its long term effects may be linked to long term rainfall variability.

This study aims at qualitatively and quantitatively assess the monthly performance of seven (TARCAT, CHIRPS, TRMM-3B43, CMORPH, PERSIANN-CDR, CMAP and GPCP) satellite derived rainfall products. The high resolution (0.05o) gridded rainfall data from ICPAC will be used to spatially evaluate the performance of each product. Wind patterns will be included in the qualitative assessments, to link the rainfall variability with satellite uncertainties.

The study reveals the following conclusive findings:

1. Rainfall over East Africa is largely controlled by large scale horizontal winds, driven by the seasonal movement of the ITCZ, and is modulated by topographic effects.
2. All satellite products assessed in this study were able to characterize rainfall patterns but have challenges on high ground areas.
3. The single sensor TARCAT rainfall product showed the lowest performance. This under-performance was especially noticeable for rain rate retrieval of orographic processes. This is attributed to its infrared single sensor that show limitation in characterizing orographic processes accurately.
4. Obviously, there is an impact of a satellite product's spatial resolution on the accuracy, at regional scale, of its rainfall estimates. Consequently, and as expected, the low spatial resolution of CMAP and GPCP leads to a failure to characterize localized rainfall variabilities. This was particularly evident for rainfall that occurred at high elevations.
5. On average, when considering all months, TRMM has the lowest errors in accuracy and precision (<15%) Consequently, TRMM is the monthly satellite rainfall product best suited for use over the region.
6. However, all products exhibited accuracy and precision errors, which have to be reduced before these products can be used in applications.

2. Materials and Methods

2.1 Datasets

A short description of the gridded rain gauge data and seven satellite derived rainfall products (TARCAT, CHIRPS, TRMM-3B43, CMORPH, PERSIANN-CDR, CMAP and GPCP), elevation and wind data are given in this section.

2.1.1 Gridded Rainfall data

Gridded rainfall data (0.05o x 0.05o) were obtained from the ICPAC regional office in Nairobi, through the Kenya Meteorological Department (KMD) (www.icpac.net). This dataset is created using interpolated, quality controlled data from 285 rain gauges over East Africa, using the inverse distance weighting method. The data were received in Band Interleaved by Line (*.bil) file format. The *.bil data were converted to *.tif, and then imported to the Integrated Land and Water Information System (ILWIS), in *.mpr format. For visualization of the processed files, the *.mpr files were exported back to *.tif format and viewed using Geographical Information System (GIS) interface in ILWIS.

Satellite data

In this study, seven satellite rainfall products were assessed, namely TARGAT, CHIRPS, TRMM-3B43, CMORPH, PERSIANN-CDR, CMAP and GPCP.

2.1.2 TARGAT

The TARGAT (TAMSAT (Tropical Applications of Meteorology using SATellite data and ground-based observations) African Rainfall Climatology and Time-series) rainfall product is a 30 year gridded TAMSAT African Rainfall Climatology derived from Meteosat thermal infrared cold cloud duration (CCD) fields and rain gauge data. Raingauge data are provided by African National Meteorological agencies. The data have a spatial resolution of 0.0375°, and a dekadal/monthly temporal resolution. TARGAT covers the African continent, and data are available from January 1983 to near present. Further details can be found in Maidment et al [15].

2.1.3 CHIRPS

The CHIRPS rainfall estimates dataset is derived from a variety of data sources which include satellite data and rain gauge data. Inputs are monthly precipitation climatology, geostationary thermal infrared data, Climate Hazards Precipitation Climatology (CHPClim), data from TRMM 3B42, precipitation data from National Aeronautics and Space Administration (NASA), atmospheric model rainfall fields from the National Oceanic and Atmospheric Administration (NOAA) Climate Forecast System, version 2 (CFSv2), and rain gauge data from a variety of sources, including regional meteorological services. The spatial resolution of the product is 0.05°, and the temporal resolution is monthly. The product covers the area between 50°N and 50°S, and data are available from January 1981 to near present. Further details can be found in Funk et al [12, 13].

2.1.4 TRMM-3B43

The TRMM-3B43 product is derived from TRMM data and the Global Precipitation Climatology Centre (GPCC) rain gauge datasets. The TRMM satellite carried five instruments, three of which are for rainfall measurements. The other two include the Clouds and Earth Radiant Energy Sensor (CERES) and Lightning Imaging Sensor (LIS). The rainfall instruments include Precipitation Radar (PR), the TRMM Microwave Imager (TMI) and the Visible and Infrared Scanner (VIRS). Several rainfall products have been developed from these sensors, the latest of which is the TRMM Multi-satellite Precipitation Analysis (TMPA) which combines several satellite products and rain gauge measurements. TRMM-3B43 is a combination of the three hourly TRMM-3B42 and monthly Global Precipitation Climatology Centre (GPCC) rain gauge analysis. The data have a spatial resolution of 0.25° and the product has a monthly temporal resolution. It covers 50°N–50°S, and data are available from January 1998 to mid-April 2015. Further details can be found in Huffman et al [1].

2.1.5 CMORPH

The CMORPH Version 1.0, is a passive microwave derived precipitation product from the National Oceanic and Atmospheric Administration (NOAA) polar-orbiting operational meteorological satellites.

The product is a combination of data derived from the United States Defense Meteorological Satellite Program (DMSP) satellites, and from the TRMM. The passive microwave instruments on board these satellites include the Advanced Microwave Sounding Unit-B (AMSU-B), the Special Sensor Microwave Imager (SSM/I), and the TRMM Microwave Imager (TMI), respectively. Infrared (IR) vector data from geostationary satellites provide interpolated estimates in the absence of passive microwave images. CMORPH has a temporal resolution of 3 hours and spatial resolution of 0.25°. It covers 60° N to 60° S, and data are available from January 1998 to near present. Further details can be found in Joyce et al [2].

2.1.6 PERSIANN-CDR

The PERSIANN-CDR dataset is derived from merging data from passive microwave sensors on board low orbiting satellites and geostationary infrared data through Artificial Neural Networks. The microwave data is derived from the TRMM microwave imager (TMI product 2A12). The geostationary geosynchronous satellite infrared imagery (GOES-IR) provides the infrared components. Three-hourly rain rate estimates are produced, which are then corrected for bias errors using GPCP (with a 2.5° resolution) monthly data, to produce daily corrected PERSIANN-CDR rainfall products. The spatial resolution is 0.25°, and the product has a daily temporal resolution. It covers 60°N–60°S and data are available from January 1983 to near present. Further details can be found in Sorooshian et al [3].

2.1.7 CMAP

The CMAP dataset is derived from several satellite products, National Center for Atmospheric Research (NCEP/NCAR) reanalysis precipitation estimates, and GPCC rain gauge data. The satellite estimates include GOES Precipitation Index (GPI), the Outgoing Longwave Radiation (OLR) based Precipitation Index (OPI), estimates from the Special Sensor Microwave/Imager (SSM/I) and estimates based on the Microwave Sounding Unit (MSU). The combined products from these sources are used to produce pentad and monthly CMAP data. The spatial resolution is 2.5°, and data are available from January 1979 to near present. The area between 90° N to 90° S is covered by the product. Further details can be found in Xie and Arkin [17].

2.1.8 GPCP

The GPCP v2.2 is developed by the World Climate Research Program (WCRP) and the Global Energy and Water Cycle Experiment (GEWEX). This product is a combination of precipitation products derived from merged satellite data and rain gauge observations. These merged data include the GPCC, microwave precipitation estimates from the SSM/I instruments and geosynchronous IR-based estimates from the Geostationary Operational Environmental Satellite (GOES) Precipitation Index (GPI) Arkin and Meisner [16]. The spatial resolution of GPCP is 2.5° and the product has a monthly temporal resolution. The area between 90° N to 90° S is covered, and data are available from January 1979 to near present. Further details can be found in Adler et al [4].

Horizontal wind data

The low level (850 mb) zonal (U) and meridional (V) wind components for the months of March, April and May, and October, November and December were downloaded from the ERA-Interim reanalysis data and computed into resultant wind vectors http://mst.nerc.ac.uk/wind_vect_convs.html (accessed December 2014).

Elevation data

Elevation data were downloaded from the Shuttle Radar Topography Mission (SRTM) 90m DEM (Digital Elevation Model) website and mosaicked over East Africa region through GIS (Geographical Information System) functionality (<http://www.cgiar-csi.org/data/srtm-90m-digital-elevation-database-v4-1>, accessed December 2014).

2.2 Methodology

2.2.1 Study Area

The study area is East Africa, located between 29° E and 42° E, and 12° S and 5° N, and comprises 5 countries, Kenya, Uganda, Tanzania, Burundi and Rwanda (Figure 1). The topography is very diverse, ranging from mountains of over 5000 m AMSL to sea level on the Indian coast.

Rainfall is highly variable in this region, in both space and time. The annual cycle is characterized by two main rainy seasons; the “long rains,” which take place from March and last through May (MAM), and the “short rains,” occurring from October to December (OND). The two seasons occur when the Inter-Tropical Convergence Zone (ITCZ) traverses the region. The ITCZ migrates from 15°S to 15°N between January and July. This leads to the ascent of air masses, cooling, condensation and precipitation from deep convective clouds [18]. This rising air descends to subtropical highs and flow back towards ITCZ, forming the meridional Hadley circulation. Convergence in the ITCZ is enhanced by a moisture influx from easterly and westerly flows during MAM and OND seasons. The easterlies occurs mainly during the transition between the Northern/Southern hemisphere summer monsoons, and are enhanced by local topographic effects. The study period is 15 years (1998–2012), which is the period during which all dataset used were available.

2.2.1 Spatial and Temporal Characteristics of Satellite Derived Rainfall Products

Both the gridded rainfall data and corresponding satellite derived rainfall estimates were each averaged for 15 years (1998–2012) for each month during the “long rains” rainy season (MAM). This was done to compare their patterns in space and time. To quantify their relationships, monthly mean errors’ standard deviations for each satellite product were determined.

Rainfall in East Africa is controlled by moisture influx, mainly from the Indian Ocean, when the ITCZ is over the Equator. To understand the linkages between wind and rainfall patterns, a qualitative comparison was carried out. The wind directions from the mean zonal and meridional wind components of ERA-Interim and converted from radians to degrees

http://mst.nerc.ac.uk/wind_vect_convts.html (accessed December 2015). First the rainfall patterns from the gridded rainfall data was compared to areas of wind convergence and high ground areas to establish how they were related.

2.2.2 Accuracy and Precision Errors of Satellite Product in relation to Gridded Rainfall Data.

Further validation was done by considering extracted satellite derived rainfall estimates and corresponding gridded rainfall data collocated at rainfall stations (284) distributed over East Africa. This was necessary to reduce the bias related to rain gauge interpolations. The relationships among the two data set were qualitatively described using scatter plots. Continuous statistics of Taylor diagrams, centered Root Mean Square Differences (RMSD), correlation coefficients (r) and Standard Deviation (σ) were used to quantify the relationships.

2.2.3 Determination of the most appropriate Satellite Product for Climate studies over East Africa.

To choose the most appropriate product for application in climate studies over East Africa, error statistics were characterized in terms of accuracy and precision. To quantify the accuracy and precision errors of each product, the percentage monthly change of their mean averages and standard deviations with respect gridded rainfall data were determined.

3. Results

March-May Rainfall Season

3.1 Spatial and temporal characteristics of satellite derived rainfall products

In this section, the gridded (0.05°) rainfall data was used to assess the monthly spatial and temporal performance of seven satellite derived rainfall products (TARCAT, CHIRPS, TRMM, CMORPH, PERSIANN CMAP and GPCP) at 0.05° scale over East Africa. Orographic rainfall retrieval is a big challenge to satellite derived rainfall products. **Figure 1 (A-C)** show rainfall patterns derived from gridded rainfall data and how they are linked to corresponding low level (850 mb) winds in **Figure 1(D-F)** and modulated by topography. The different colours of the wind vectors show change in wind directions and their arrows point in the direction of the flow. It is clear that easterlies to south easterlies lead to increased rainfall over areas of wind convergence and on high ground areas (e.g. Mount Kenya of the central Kenya highlands). Rainfall variability show dependence on low level wind flow orientations and this is because of the moisture they influx from the Indian Ocean. For example, during rainfall onset in March the easterlies enhances rainfall over southern part of the region (Tanzania, Rwanda and Burundi). However, it can be observed that the same is blocked by Kenya highlands and turn south east –north west orientation (Turkana low level jet)[14, 19]. This explains the low orographic processes around Mount Kenya during this month and a general rainfall reduction over most parts of Kenya. In April the wind flow is generally south easterlies and causes increased rainfall over the region. It can be observed that during the month of May, the south easterlies are still dominant, but divergence over the central highlands of Kenya reduces orographic rainfall processes.

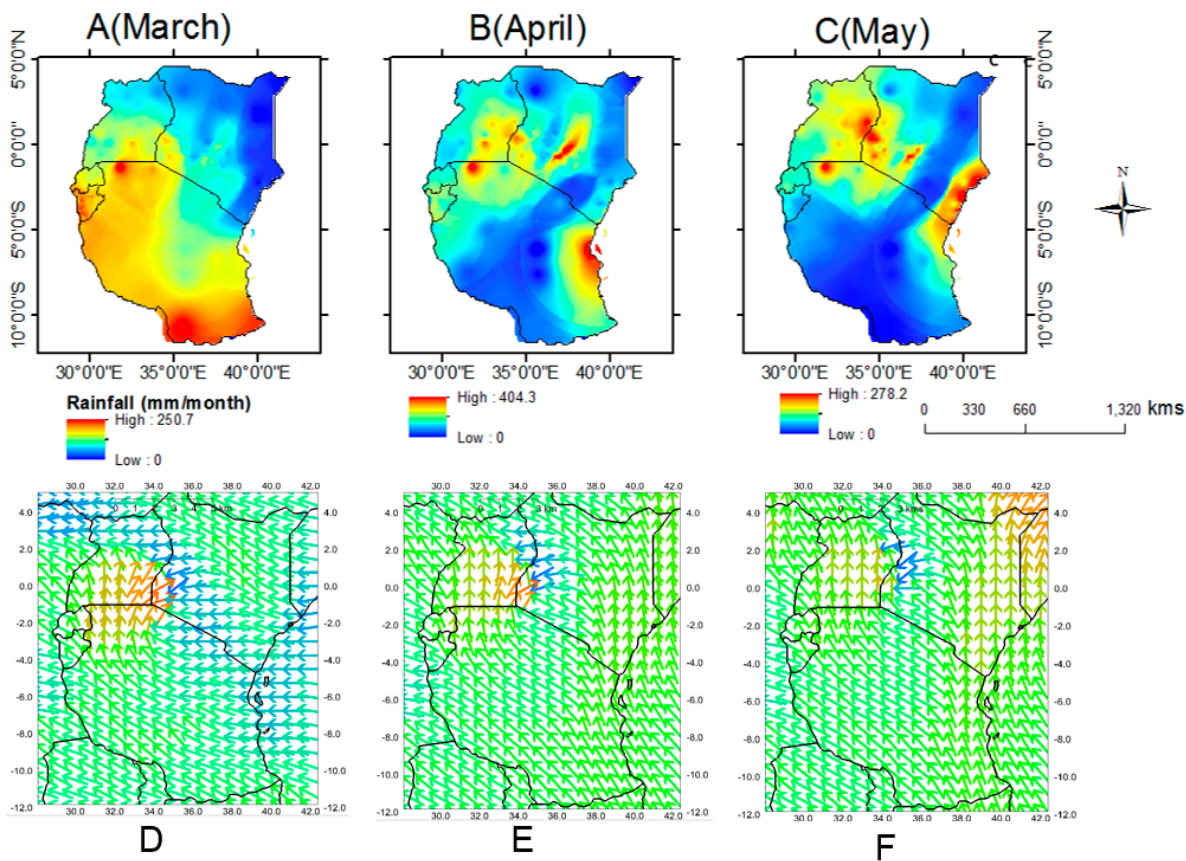


Figure 1 (A–C) show Mean (1998–2012) gridded rainfall data for March –May months and the corresponding wind patterns in Figure 1 (D–F) from Era-Interim zonal and meridional wind data. The different colors show changes in mean wind direction.

Figure 2 shows the monthly mean (1998–2012) rainfall patterns of both satellite derived rainfall products and the corresponding gridded rainfall data. It can be observed that the two datasets agree well in retrieving spatial rainfall patterns, apart from over the high ground areas, particularly the Mount Kenya region.

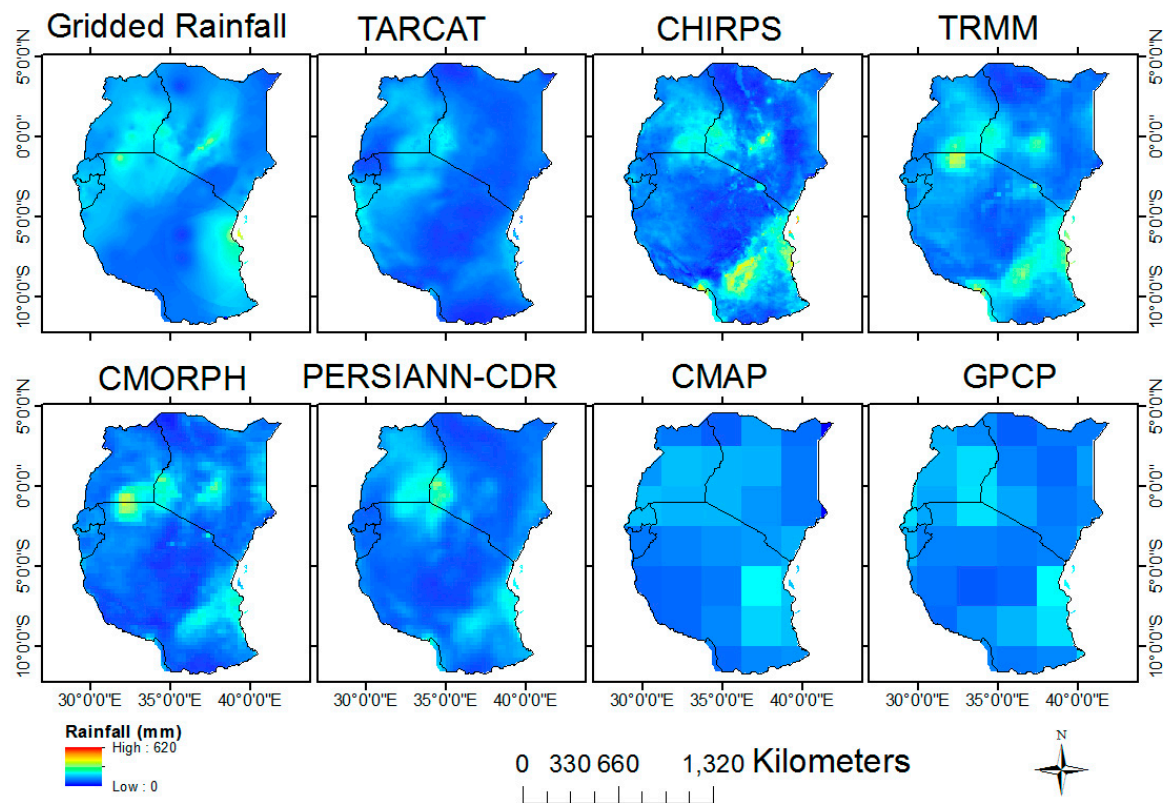


Figure 2: Monthly mean satellite rainfall estimates and gridded rainfall data for the peak rainfall month of April, during the MAM rainy season.

The error distribution of the satellite products, relative to the gridded rainfall data, is shown in Figure 3. Evidently, all seven products have highest errors distributed over the high ground areas and the Lake Victoria region (located around the Kenya, Tanzania and Uganda border areas). April is the peak month of March-May rainfall season and it is clear the products have challenges in retrieving high rainfall intensities. Again, errors are also observed over mountainous areas, indicated some challenges in the retrieval of orographic rainfall.

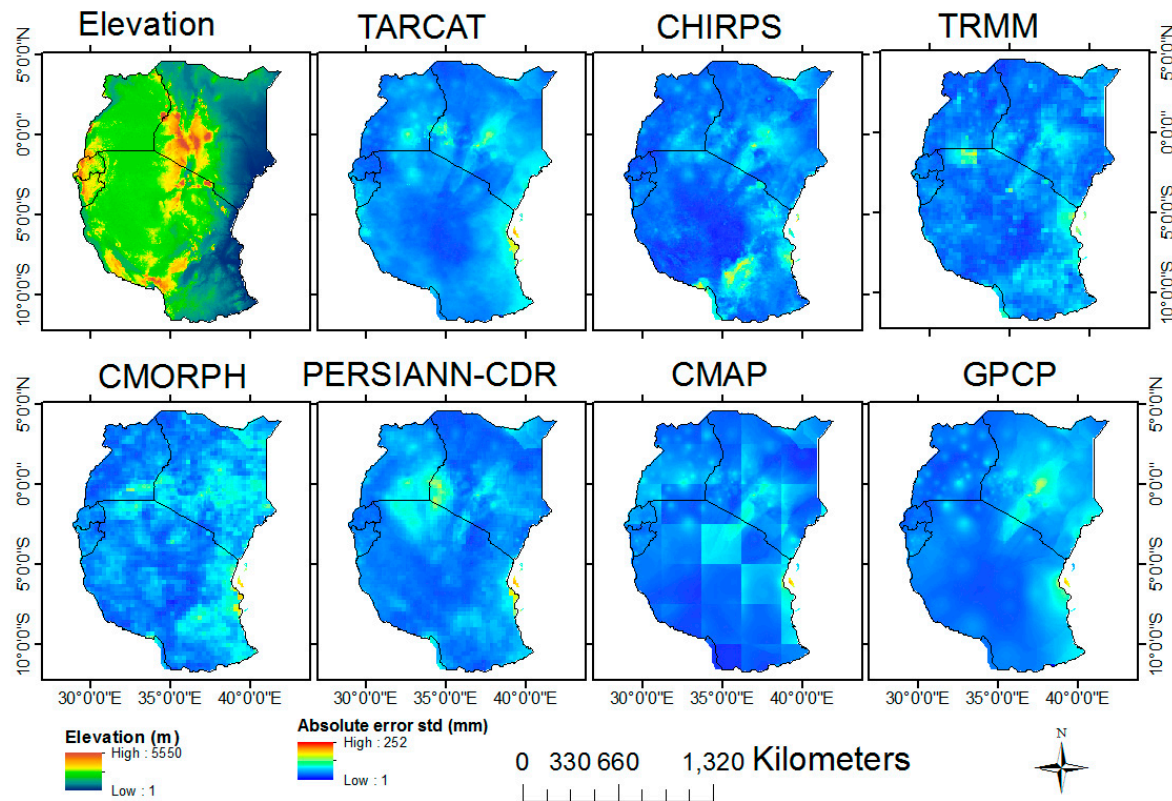


Figure 3: Monthly mean (1998-2012) satellite derived rainfall estimates' mean errors' standard deviations during the month of April.

3.2 Temporal and spatial accuracy and precision errors

In this section, the mean (1998-2012) monthly satellite derived rainfall estimates and the corresponding gridded rainfall data collocated at the raingauge stations (284) were used for validation. Use of stations' locations were used to minimise errors related to sparse rain gauge distributions during interpolation.

Figure 4 show scatter plots, comparing each of the the satellite products to gridded rainfall data during March -May months. It can be observed that each of the products shows close correspondence with gridded rainfall data during rainfall onset (March) when monthly rainfall intensity is low. However, their performance decreases with increase (~200 mm month⁻¹) in rainfall intensity in April and May as indicated by a general decrease in coefficient of determinations (R^2) by all products. TARCAT, PERSIANN, CMAP and GPCP show the lowest performance with $R^2 < 0.3$. Conversely, CHIRPS, TRMM and CMORPH have good performance indicated by $R^2 \geq 0.6$. TRMM rainfall retrieval is good in areas of varying rainfall variabilities[20] including the mountainous areas and this explains its highest performance over this region.

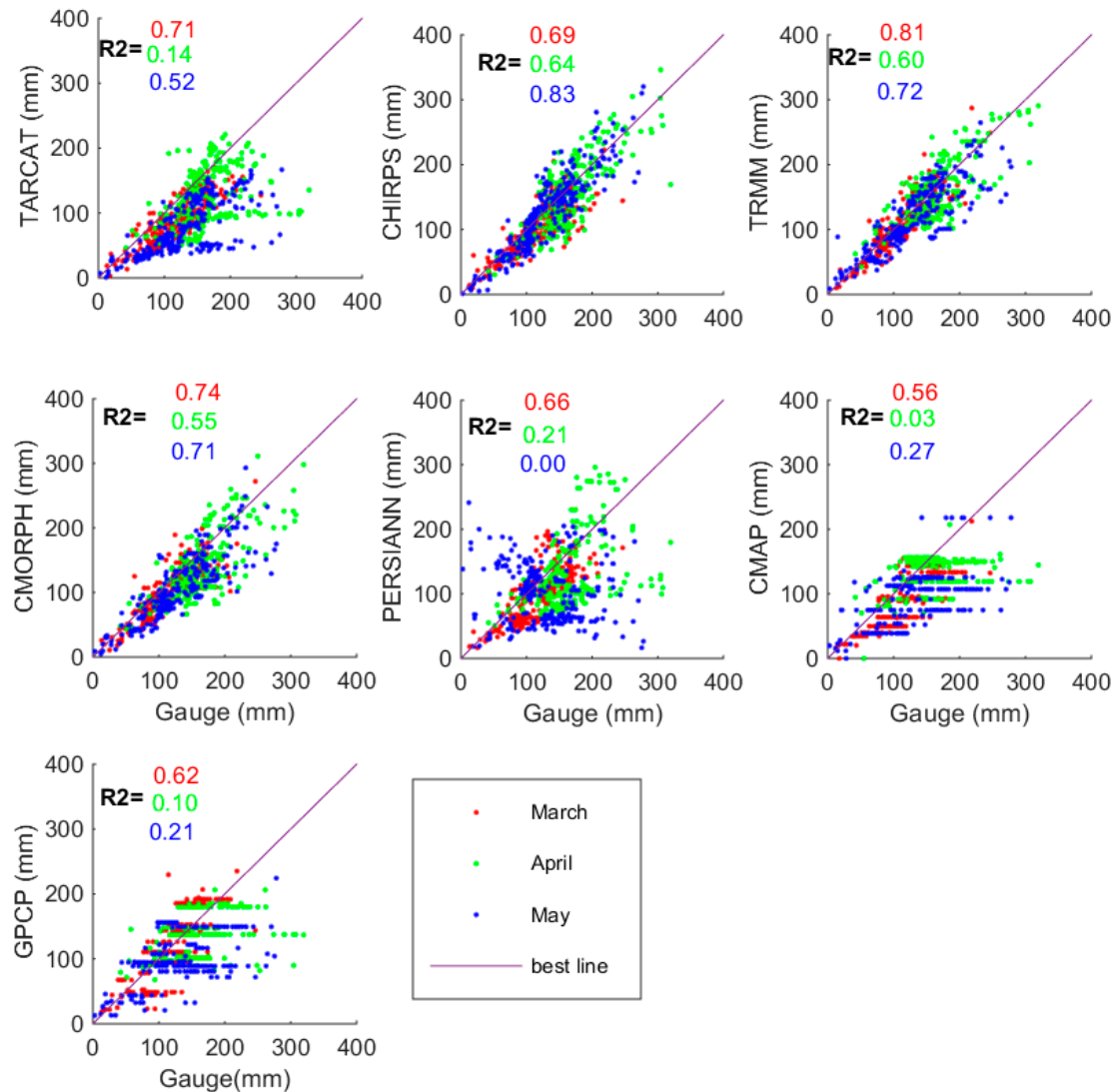


Figure 4: Scatter plots of the monthly mean (1998-2012) satellite derived rainfall estimates in relation to the corresponding raingauge observations over 284 rainfall stations during March–May rainfall months.

These results are in agreement with results of a recent study carried out over West Africa where seven satellite rainfall products were evaluated at different timescales [20]. They evaluated CHIRPS, TARCAT, PERSIANN, African Rainfall Estimation (RFE 2.0), and TRMM (3B42, 3B43) and Africa Rainfall Estimate Climatology (ARC 2.0). The results showed overestimations by most products when monthly rainfall was over 200 mm. Furthermore, they found that performance decreased with an increase in spatial scales [21]. This is similar to Maggioni et al [22] findings that relative bias doubles from rainfall to run off across all basin scales indicating the impact of an increase in spatial scale. In this study, similar results have been found. CMAP and GPCP performance is reduced, due to their coarse spatial scale. Figure 5 shows the Taylor diagrams, describing the monthly performance of satellite rainfall estimates in relation to the gridded rainfall data across East Africa during the MAM rainy season. Concurring with previous findings, it can be observed that the performance of all satellite products is low when rainfall intensity is high, i.e. during the months of April and May. CHIRPS, CMORPH and TRMM have good performance in the three months, indicated by correlation coefficient > 0.7 , lowest root squared mean error and low standard deviations. Conversely, TARCAT, PERSIANN, CMAP and GPCP showed poor performance. As previously observed, the differences in their performance arise from the failure to correctly estimate orographic rainfall.

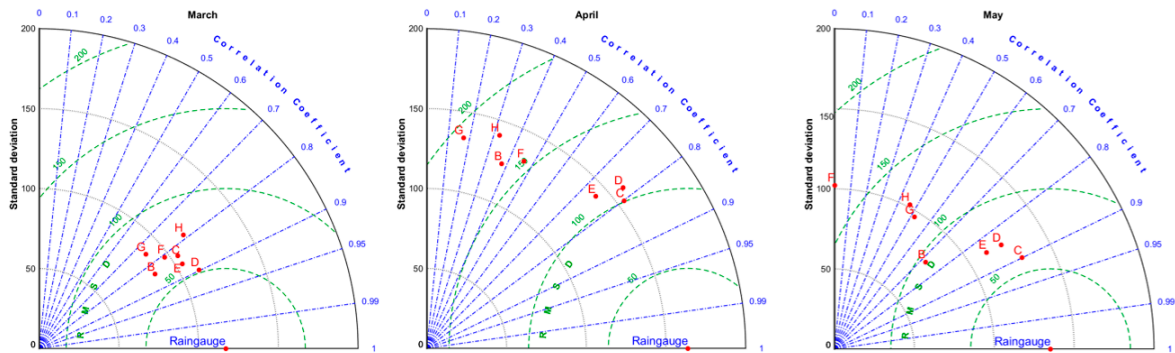


Figure 5: Taylor diagrams displaying a statistical comparison of gridded (0.05o) raingauge data with seven satellite derived rainfall products (TARCAT: B, CHIRPS (C), TRMM (D), CMORPH (E), PERSIANN (F), CMAP (G) and GPCP (H) for a period of fifteen years (1998-2012) on monthly basis of the wet months of March-May.

3.3 Determination of the most appropriate satellite product for climate applications over East Africa – MAM rainy season.

In this section, monthly means and standard deviations (1998-2012) of each satellite derived rainfall product are computed. Table 1 shows the error summaries, classified in terms of accuracy and precision respectively. It is evident that TARCAT, PERSIANN, CMAP and GPCP have the highest overall errors, and CHIRPS, TRMM and CMORPH have the lowest errors. Overall, TRMM shows the best performance.

Table 1. Mean (1998-2012) satellite derived rainfall estimates’ percentage accuracy and precision errors, in relation to the gridded rainfall data, during MAM rainfall season

Products	March		April		May	
	Accuracy	Precision	Accuracy	Precision	Accuracy	Precision
TARCAT	-12	-26	1	-24	-27	-42
CHIRPS	-3	-11	23	-6	12	-3
TRMM	4	-4	7	-3	-8	-9
CMORPH	1	-11	12	-13	-4	-17
PERSIANN	8	-17	32	-19	-16	-24
CMAP	4	-24	-43	-18	-31	-29
GPCP	30	-2	-31	-14	-32	-25

October-December Rainfall Season

3.4 Spatial and temporal characteristics of satellite derived rainfall products

In this section, the spatial and temporal performance of mean monthly satellite derived rainfall estimates, calculated over a 15 year period (1998 – 2012), is assessed for the OND rainy season. The topographic influence on low level moisture influx is more evident during this season, and consequently orographic induced uncertainties of satellite estimates are more evident. In Figure 6 (A-C) gridded rainfall data indicate decreased rainfall to the southern part of the region (Tanzania) in October, as south easterly winds turns easterly over Tanzania, Rwanda and Burundi in Figure 6 (D). The low level (850 mb) south-easterlies and south westerlies winds diffluence is dominant during this season (Figure 6 (D-F)) and reduce rainfall amounts over the region. However, the south-easterlies enhances orographic processes [19, 23] over Mount Kenya of the central Kenya highlands,

causing increased monthly rainfall intensities. However, as found during the MAM rainy season, the performance of most satellite rainfall retrieval products is fairly poor in accurately estimating this orographic rainfall. In December the north easterly winds become more dominant (Figure (F)) increasing low level divergence and reducing moisture influx to the Kenya highlands. Over Uganda, south-easterly winds turns northerly through to Rwanda and Burundi, causing increased rainfall. This shows the influence of the general circulation and topography to East Africa rainfall distribution particular during this season.

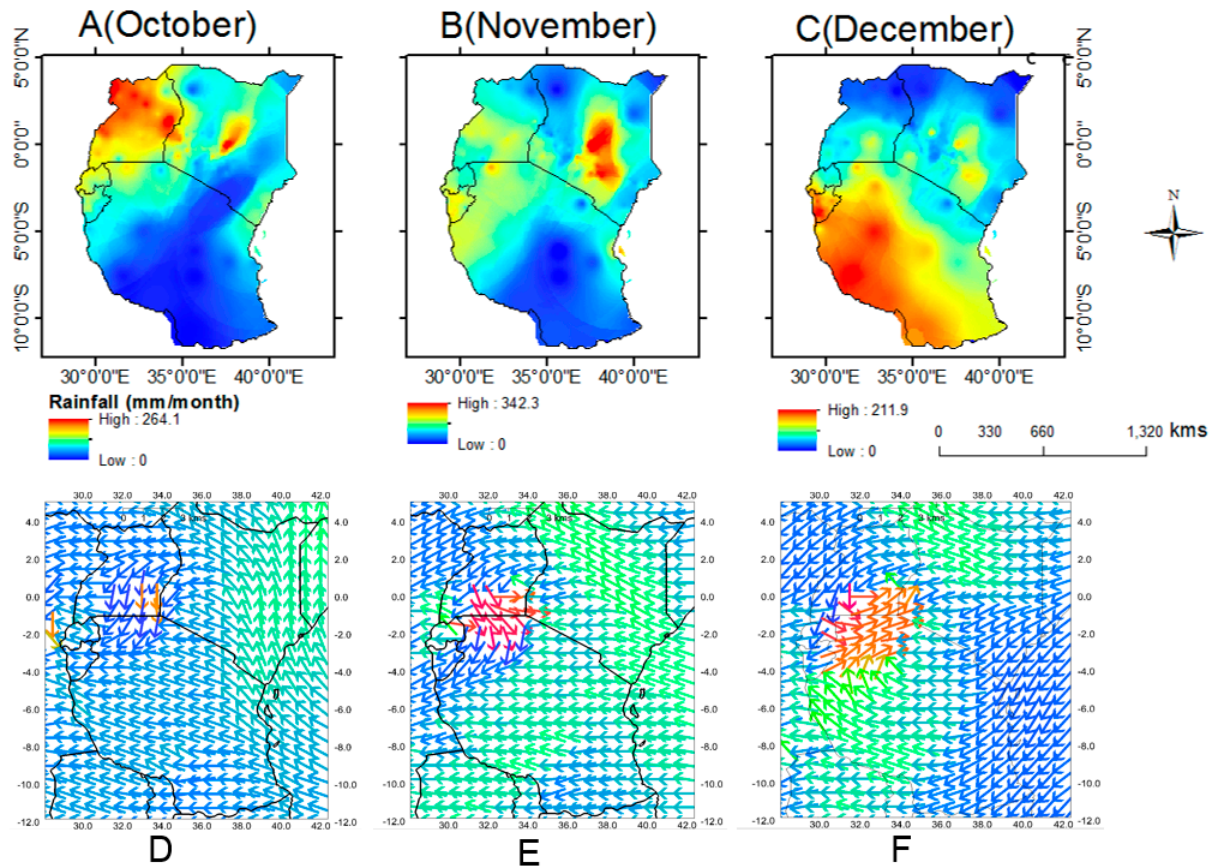


Figure 6 (A-C) show Mean (1998-2012) gridded rainfall data for October –December months and the corresponding wind patterns in Figure 6 (D-F) from Era-Interim zonal and meridional wind data. The different colors show changes in mean wind direction.

From Figure 7, it can be observed that TARCAT and PERSIANN products have low skills in retrieving rainfall generated by orographic processes in November, which is the peak month of the season.

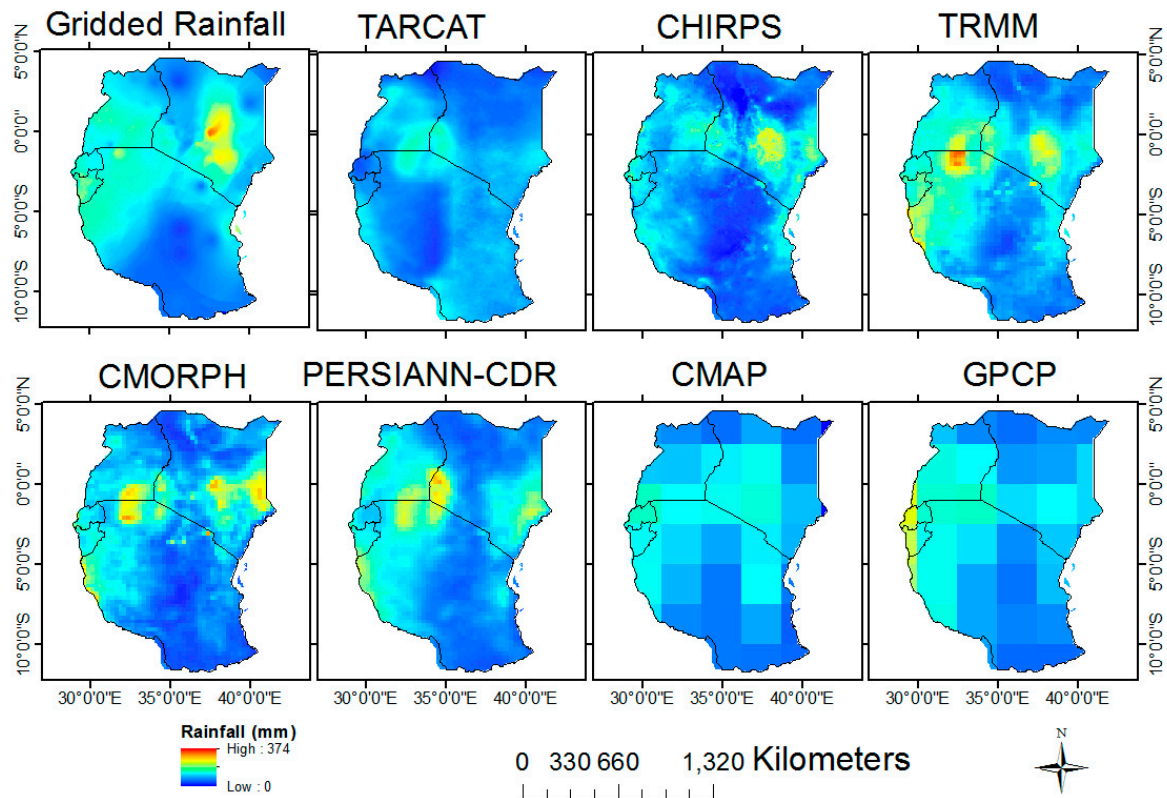


Figure 7: Mean (1998-2012) Mean Satellite rainfall estimates and corresponding gridded rainfall data during the peak rainfall month of November (OND rainfall season).

Likewise, the coarse resolution products (CMAP and GPCP) show low skills over same areas. Figure 8 show how the satellite products' errors are concentrated over the high ground areas, indicating that although they differ in rain rate retrieval skills, all products have difficulties in accurately retrieving orographic rainfall.

TARCAT, PERSIANN, CMAP and GPCP show the lowest rain rate retrieval skills, similar to what was found during the MAM rainy season. Again, the largest discrepancies between the satellite products and the gridded rainfall dataset were found over the Kenyan highlands.

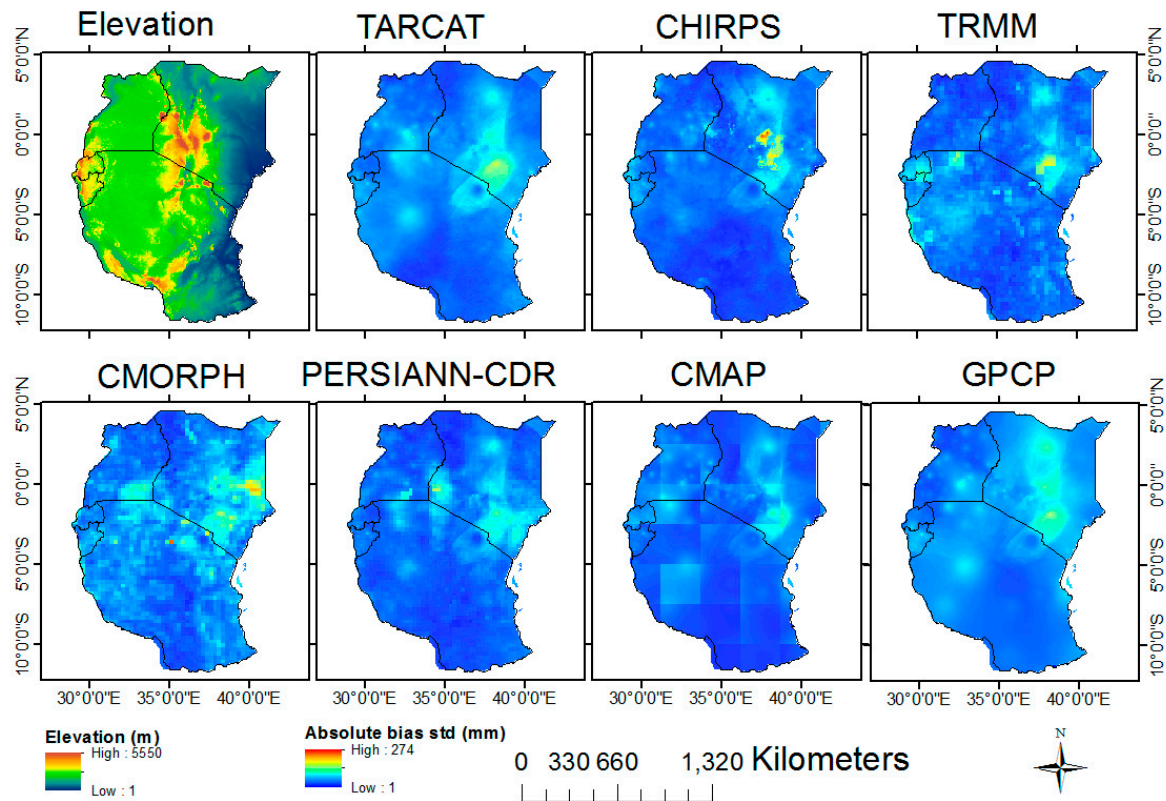


Figure 8: Monthly mean (1998-2012) satellite derived rainfall estimates' mean errors' standard deviations during the month of November (1998 – 2012 averages).

3.5 Spatial and temporal accuracy and precision errors.

Validation was done using monthly mean rainfall data, calculated over a period of 15 years (1998-2012).

A general decrease in products' performance is evident from decreased R^2 (Figure 9) and low linearity in the scatter plots. It is clearly shown that CHIRPS, TRMM and CMORPH products have the closest correspondence with the rain gauge data, as also found during the MAM rainy season. TARCAT and PERSIANN again show the lowest performance. This is indicated by a very low R^2 (<0.1) during the month of November, and a general poor correspondence with the rain gauge data.

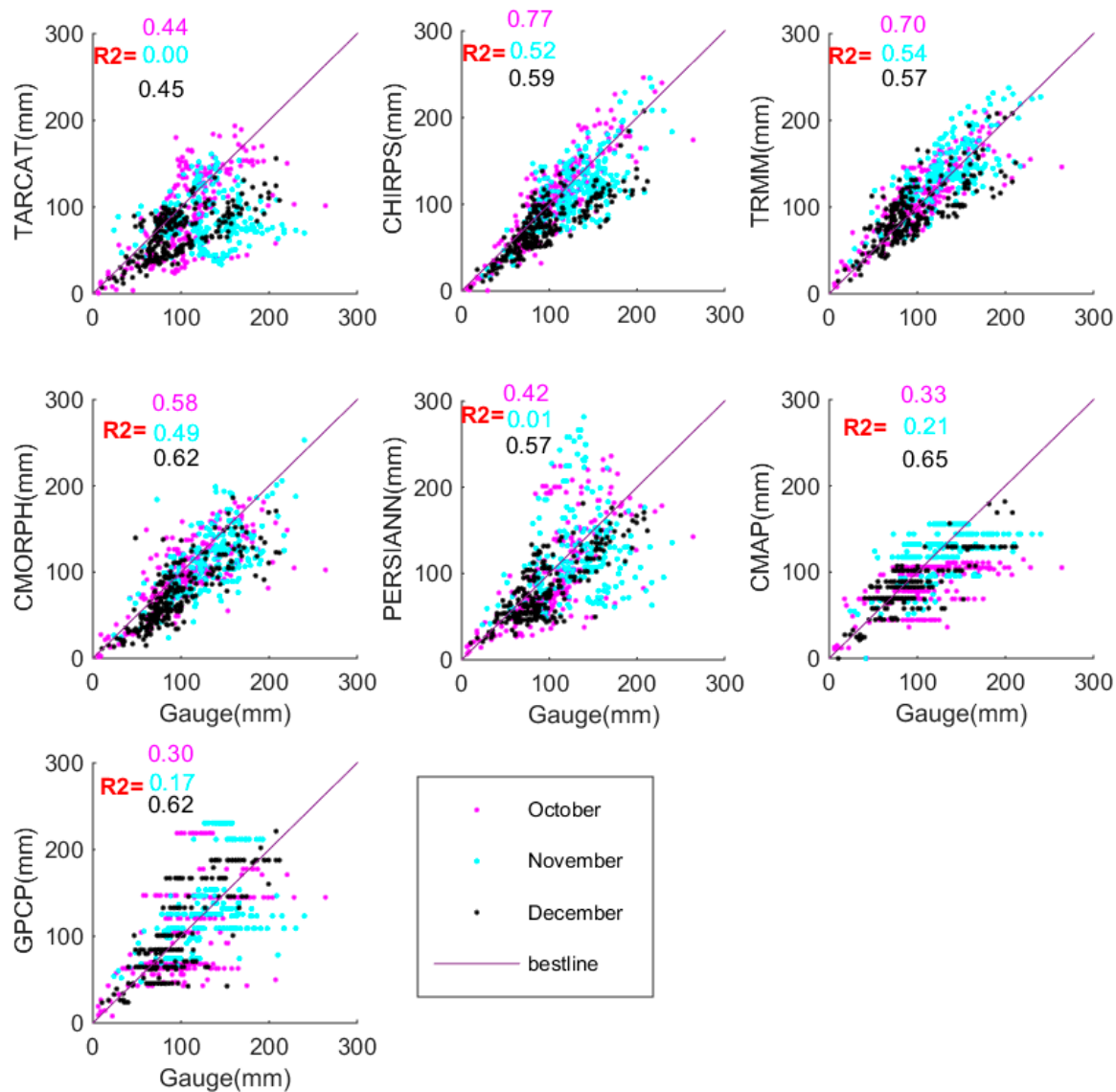


Figure 9: Scatter plots of the monthly mean (1998–2012) satellite derived rainfall estimates in relation to the corresponding raingauge observations over 284 rainfall stations during October–December rainfall months.

The Taylor diagrams in Figure 10 show the error statistics of the satellite rainfall products in relation to the gridded rainfall data. Results concur with March–May rainfall season's findings, showing the lowest products' performance during the month of November, which is the peak rainfall month of the OND rainy season. Even though the OND rainy season has less rainfall than the MAM rainy season, the satellite products performance is poorer during the OND rains, demonstrated by the minimum values of the correlation coefficients (0.7 in March, versus 0.5 in October). This shows that the performance of the satellite products is not only influenced by the rainfall intensity per se, but also by the rainfall regimes. CHIRPS, CMORPH and TRMM have lowest RMSD, i.e. rainfall estimates are nearest to the gridded rainfall data. TARCAT, PERSIANN, CMAP and GPCP show the poorest performance during the OND rainy season.

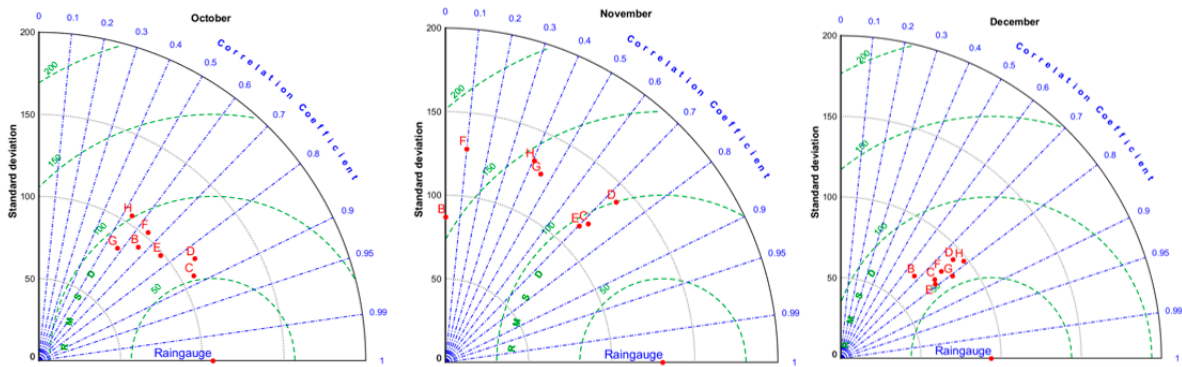


Figure 10: Taylor diagrams displaying a statistical comparison of gridded (0.05o) rainfall data with the satellite derived rainfall products (TARCAT: B, CHIRPS (C), TRMM (D), CMORPH (E), PERSIANN (F), CMAP (G) and GPCP (H) for a period of fifteen years (1998–2012) on monthly basis of the wet months of October–December.

3.6 Determining the most appropriate satellite product for climate applications over East Africa – OND rainy season.

To determine the best performing satellite rainfall product during the OND rainy season, mean errors in terms of accuracy and precision were derived from the percentages of each satellite rainfall product’s mean and standard deviation relative to the gridded rainfall data. It is clearly evident from Table 2 that TARCAT has errors >15% during each month in the OND rainy season, indicating poor rain rate retrieval skills during this season. PERSIANN, CMAP and GPCP have the overall highest (~>20 %) percentage of errors. TRMM again shows the best performance, with the lowest errors. From these results it is clear that the satellite rainfall products are affected by both errors in accuracy and precision, resulting in both a low rain rate retrieval skill and poor spatial characterization of the rainfall.

Table 2: Mean (1998–2012) satellite derived rainfall estimates’ percentage accuracy and precision errors, in relation to the gridded rainfall data, during OND rainfall season

Products	October		November		December	
	Accuracy	Precision	Accuracy	Precision	Accuracy	Precision
TARCAT	17	-14	-20	-34	-29	-27
CHIRPS	15	1	-3	-9	-20	-19
TRMM	-2	7	-9	7	-13	-1
CMORPH	-4	-8	-2	-12	-8	-20
PERSIANN	44	-3	51	-2	-6	-12
CMAP	-39	-22	-34	-3	-28	-8
GPCP	31	-1	23	1	26	4

4. Discussion

This study presents spatial and temporal assessments of seven satellite derived rainfall products in relation to the gridded rainfall data over East Africa. Topography affects the performance of satellite rainfall products [2, 4, 20] and this impacts are seasonal dependant and varies from product to product. Understanding the underlying cause of this seasonality is important regional wise is important. Figure 1 shows low level (850 mb) wind flow and its links to convective and orographic rainfall, the former indicated by wind convergence and corresponding rainfall occurrence during the MAM rainfall season. In the vicinity of high ground areas with a wind ward orientation, shown in

Figure 1 (4) and (5), orographic processes are enhanced. The use of data from infrared sensors for rainfall retrieval relates cold clouds to high rainfall rates [15], but over mountainous areas, warm cloud orographic processes drive most of the rainfall. Consequently, IR based satellite products underestimate rainfall over high ground areas. This is confirmed by the findings in this study. The single infrared sensor products [10] show the lowest performance in retrieving orographic rainfall. For example, TARGAT uses only infrared data and had the lowest performance on mountainous areas. It is good to note that the inclusion of ground data in the TARGAT algorithm is not sufficient to overcome the drawbacks inherent in single sensor algorithms. Similarly, PERSIANN shows low performance on high ground areas [20], even though it combines infrared and passive microwave derived data. The reason for this is that its main input is infrared and the algorithm only uses data from passive microwave sensors for training the neural network [21].

Subpixel rainfall variabilities could not be characterized by the coarse resolution products (CMAP and GPCP) and resulted in high underestimations of localized high rainfall. This mainly affected the high ground areas where a single pixel covers areas with high and low elevation. However, products of similar spatial scales differed in performance. This is mainly due to their input data differences. For example, GPCP and CMAP performance is high at low rainfall accumulation (< 150 mm) but CMAP perform better than GPCP when rainfall amount exceed 200 mm [21]. CMAP using Infrared and passive sensors for rainfall retrieval [17], while GPCP uses mainly data from infrared sensors [4]. Also, the huge offset differences in their locations and the fact that rainfall over the region varies within a small distance may have contributed to their differences. TRMM uses infrared and passive microwave data in rainfall retrieval and satellite borne radar hence its high performance on mountainous areas [22]. Consequently, CHIRPS, and CMORPH inclusion of TRMM estimates may be attributed to their good performance over those areas. Further study by, Liu et al[23] found that rainfall intensity is an important factor affecting the performance of satellite rainfall estimates. Those findings concur with the results shown in Figure 4. The satellite products showed a significant underestimation of high (≥ 200 mm month⁻¹) rainfall intensities, as observed during the peak rainfall month of April. Although during the peak month (November) of the OND rainfall season, monthly rainfall was low compared to April (Figure 9), the performance of all satellite products was lower. This arises from the rainfall regime that is dominant in a given season. During the MAM season, as shown earlier (Figure 1), and the south easterlies during OND season, convective activities decrease and orographic processes are dominant. The decreased convective activities reduces the performance of satellite products and southeasteries convergence enhances convective rainfall which is favorable for infrared sensors applied for rainfall retrieval. Conversely, during OND rainfall season, orographic processes are dominant as south westerlies are suppressed by northerly flow during southern Hemisphere summer. The performance of satellite products decreases as the convections become shallower and warmer orographic process increases.

5. Conclusions

Satellite derived rainfall products are useful supplements to sparse rain gauge networks for use in climate studies and water resources management, to mention a few applications. Although satellite rainfall products have been evaluated globally and to some extent regionally, there are significant variations in their performance, especially due to geographical location, climate and rainfall regime. Certain products will have advantages over other products in some regions or climates, whilst other products might be more appropriate for use in other climates or regions. There is therefore a need to quantify their uncertainties before selecting the appropriate product for the region. In this study, seven satellite derived rainfall products (TARGAT, CHIRPS, TRMM, CMORPH, PERSIANN CMAP and GPCP) of different spatial scales are assessed spatially and temporally using gridded (0.05°) rainfall data over East Africa for 15 years (1998-2012). All the products were converted to monthly temporal and 0.05° spatial scales. To aid understanding of the performances of the products spatially and temporally, corresponding mean wind patterns for each month during the rainy season, as well as a digital elevation model of the region were used.

The findings of this study are as follows.

1. Rainfall over East Africa is largely controlled by large scale horizontal winds, driven by the seasonal movement of the ITCZ, modulated by topographic effects.
2. All satellite products assessed in this study were largely able to characterize rainfall patterns. But most products were shown to have difficulties in accurately estimating rainfall over areas of high elevation.
3. The single sensor TARGAT rainfall product showed the poorest performance. This under-performance was especially noticeable for rain rate retrieval of orographic processes. This is attributed to its use of a single infrared sensor. Whereas the use of IR satellite data offers certain advantages, notably in terms of temporal and spatial resolution, such data are less suited for rain rate retrieval for orographic clouds, which are relatively warm and caused primarily by kinetic turbulence, rather than convection.
4. Obviously, there is an impact of a satellite product's spatial resolution on the accuracy, at regional scale, of its rainfall estimates. Consequently, and as expected, the low spatial resolution of CMAP and GPCP leads to a failure to characterize localized rainfall variabilities. This was particularly evident for rainfall that occurred at high elevations.
5. On average, when considering all months, the monthly rain rates derived from TRMM have the lowest errors in accuracy and precision (<15%). Consequently, TRMM is the satellite rainfall product best suited for use over the region. The high performance of TRMM is attributed to its multi-sensor use in rainfall retrieval that includes passive microwave and space borne radar. This enables it to characterize rainfall of different regimes.
6. However, all products exhibited accuracy and precision errors, which have to be reduced before these products can be used in applications.

Ongoing work will focus on reducing the uncertainties of the satellite derived rainfall estimates to improve their applicability.

Acknowledgments

This work was made possible through the funding provided by Netherlands Fellowship Programmes (NFP), and we greatly appreciate that offer. The University, provides funds for open access.

Author Contributions

All the three author contributed in concept building and manuscript preparations. Kimani analyzed the data and drafted the manuscript. Su and Hoedjes provided conceptual advice and contributed the over all writing and approval of the final manuscript.

Conflicts of Interest

The authors declare no conflict of interest.

References

- [1] C. Kidd, P. Bauer, J. Turk, G. J. Huffman, R. Joyce, K. L. Hsu, et al., "Intercomparison of High-Resolution Precipitation Products over Northwest Europe," *Journal of Hydrometeorology*, vol. 13, pp. 67-83, Feb 2012.

- [2] R. J. Joyce, J. E. Janowiak, P. A. Arkin, and P. P. Xie, "CMORPH: A method that produces global precipitation estimates from passive microwave and infrared data at high spatial and temporal resolution," *Journal of Hydrometeorology*, vol. 5, pp. 487-503, Jun 2004.
- [3] S. Sorooshian, K. L. Hsu, X. Gao, H. V. Gupta, B. Imam, and D. Braithwaite, "Evaluation of PERSIANN system satellite-based estimates of tropical rainfall," *Bulletin of the American Meteorological Society*, vol. 81, pp. 2035-2046, Sep 2000.
- [4] R. F. Adler, G. J. Huffman, A. Chang, R. Ferraro, P. Xie, J. Janowiak, et al., "The Version 2 Global Precipitation Climatology Project (GPCP) Monthly Precipitation Analysis," *J. Hydrometeorol.*, vol. 4, pp. 1147-1167, 2003.
- [5] H. Feidas, K. Lagouvardos, V. Kotroni, and C. Cartalis, "Application of three satellite techniques in support of precipitation forecasts of a NWP model," *International Journal of Remote Sensing*, vol. 26, pp. 5393-5417, Dec 20 2005.
- [6] T. Dinku, P. Ceccato, E. Grover-Kopec, M. Lemma, S. J. Connor, and C. F. Ropelewski, "Validation of satellite rainfall products over East Africa's complex topography," *International Journal of Remote Sensing*, vol. 28, pp. 1503-1526, Apr 2007.
- [7] Z. D. Adeyewa and K. Nakamura, "Validation of TRMM radar rainfall data over major climatic regions in Africa," *Journal of Applied Meteorology*, vol. 42, pp. 331-347, Feb 2003.
- [8] J. E. Diem, J. Hartter, S. J. Ryan, and M. W. Palace, "Validation of Satellite Rainfall Products for Western Uganda," *Journal of Hydrometeorology*, vol. 15, pp. 2030-2038, Oct 2014.
- [9] F. Mashingia, F. Mtalo, and M. Bruen, "Validation of remotely sensed rainfall over major climatic regions in Northeast Tanzania," *Physics and Chemistry of the Earth*, vol. 67-69, pp. 55-63, 2014.
- [10] T. Dinku, P. Ceccato, and S. J. Connor, "Challenges of satellite rainfall estimation over mountainous and arid parts of east Africa," *International Journal of Remote Sensing*, vol. 32, pp. 5965-5979, 2011.
- [11] C. Funk, P. Peterson, M. Landsfeld, D. Pedreros, J. Verdin, S. Shukla, et al., "The climate hazards infrared precipitation with stations—a new environmental record for monitoring extremes," *Scientific Data*, vol. 2, p. 150066, 12/08/online 2015.
- [12] C. C. Funk, P. J. Peterson, M. F. Landsfeld, D. H. Pedreros, J. P. Verdin, J. D. Rowland, et al., "A quasi-global precipitation time series for drought monitoring: U.S. Geological Survey Data Series 832, 4 p.," 2014.
- [13] C. Funk, S. E. Nicholson, M. Landsfeld, D. Klotter, P. Peterson, and L. Harrison, "The Centennial Trends Greater Horn of Africa precipitation dataset," *Scientific Data*, vol. 2, p. 150050, 09/29/online 2015.
- [14] S. Nicholson, "The Turkana low-level jet: mean climatology and association with regional aridity," *International Journal of Climatology*, vol. 36, pp. 2598-2614, May 2016.
- [15] R. I. Maidment, D. Grimes, R. P. Allan, E. Tarnavsky, M. Stringer, T. Hewison, et al., "The 30 year TAMSAT African Rainfall Climatology And Time series (TARCAT) data set," *Journal of Geophysical Research-Atmospheres*, vol. 119, pp. 10619-10644, Sep 2014.

- [16] G. J. Huffman, R. F. Adler, D. T. Bolvin, G. J. Gu, E. J. Nelkin, K. P. Bowman, et al., "The TRMM multisatellite precipitation analysis (TMPA): Quasi-global, multiyear, combined-sensor precipitation estimates at fine scales," *Journal of Hydrometeorology*, vol. 8, pp. 38-55, Feb 2007.
- [17] P. Xie and P. A. Arkin, "Global monthly precipitation estimates from satellite-observed Outgoing Longwave Radiation," *J. Climate*, vol. 11, , pp. 137-164., 1997.
- [18] T. Schneider, T. Bischoff, and G. H. Haug, "Migrations and dynamics of the intertropical convergence zone," *Nature*, vol. 513, pp. 45-53, Sep 2014.
- [19] J. H. Kinuthia and G. C. Asnani, "A NEWLY FOUND JET IN NORTH KENYA (TURKANA CHANNEL)," *Monthly Weather Review*, vol. 110, pp. 1722-1728, 1982.
- [20] X. H. Li, Q. Zhang, and C. Y. Xu, "Assessing the performance of satellite-based precipitation products and its dependence on topography over Poyang Lake basin," *Theoretical and Applied Climatology*, vol. 115, pp. 713-729, Feb 2014.
- [21] M. R. P. Sapiano, "An evaluation of high resolution precipitation products at low resolution," *International Journal of Climatology*, vol. 30, pp. 1416-1422, Jul 2010.
- [22] L. K. Ning, H. L. Liu, A. M. Bao, and X. L. Pan, "Adaptability evaluation of TRMM over the Tianshan Mountains in central Asia," *Mausam*, vol. 67, pp. 625-632, Jul 2016.
- [23] H. Liu, S. Sorooshian, and X. Gao, "Assessment of the Spatial and Seasonal Variation of the Error-Intensity Relationship in Satellite-Based Precipitation Measurements Using an Adaptive Parametric Model," *JOURNAL OF HYDROMETEOROLOGY*, vol. 16, pp. 1700-1716, 2015.



© 2016 by the authors; licensee *Preprints*, Basel, Switzerland. This article is an open access article distributed under the terms and conditions of the Creative Commons by Attribution (CC-BY) license (<http://creativecommons.org/licenses/by/4.0/>).